Visualisierung der 2-Phasen-Strömung in einer PEM-Elektrolyse-Zelle durch Neutronentomographie

Visualization of the two-phase-flow inside a running polymer electrolyte membrane water electrolysis cell using neutron radiography

Alexander Spies[1,6*], Michael A. Hoeh[2], Tobias Arlt[3] , Nikolay Kardjilov[3], David L. Fritz[2], Jannik Ehlert[2], John Banhart[3,4], Manuel Münsch[6], Antonio Delgado[6], Alexander Hahn[1], Ingo Manke[3], Werner Lehnert[2,5]

[1] Siemens AG, Hydrogen Solutions, 91052 Erlangen
[2] Forschungszentrum Jülich GmbH, Institute of Energy and Climate Research, IEK-3: Electrochemical Process Engineering, 52425 Jülich, Germany
[3] Helmholtz-Zentrum Berlin GmbH, Institute of Applied Materials, Hahn-Meitner-Platz 1, 14109 Berlin, Germany
[4] Technische Universität Berlin, Hardenberg Str. 36, 10623 Berlin, Germany
[5] Modeling in Electrochemical Process Engineering, RWTH Aachen University, 52056 Aachen, Germany
[6] Institute of Fluid Mechanics, Friedrich-Alexander-Universität Erlangen-Nürnberg, 91058 Erlangen
*corresponding author, alexander.spies@siemens.com

Elektrolyse, PEM, Gasdiffusionsschicht, 2-Phasen-Strömung, Neutronen-Radiographie
Electrolysis, PEM, gas diffusion layer, 2-phase flow, neutron radiography

Abstract

With the rising fraction of renewable energy sources on the overall electricity production – especially in Germany – the load leveling of electric energy due to the volatile character of renewable energy sources compared to conventional energy sources like coal or natural gas becomes more and more important. One possibility to store electrical energy short term and also over a duration of days and weeks is to convert the energy to hydrogen by electrolysis. Especially PEM[1]-electrolysis offers a high flexibility and at the same time a high purity of the produced hydrogen. One of the core components of a PEM-electrolysis cell is the gas diffusion layer (GDL, also referred to as the current collector or porous transport layer in the literature), which enables the distribution of the electric current and at the same time supports the removal of the evolving gases. Due to high current densities during cell operation massive metal structures are necessary and it is not possible to visually observe the 2-phaseflow processes inside of the cell without disturbing the flow field or the distribution of the electric current. One possibility to gain an insight into a running cell is the usage of neutron radiography. In the following work the two-phase flow at different operating conditions was examined and results are discussed. Influences of different cell conditions on the point of operation are being documented, too.

---

[1] PEM = Polymer Electrolyte Membrane

1. Introduction

Water electrolysis has been a field of growing interest in the recent years due to its ability to store electricity generated from intermittent renewable sources like wind or solar energy. In this way it is possible to store larger amounts of energy compared to other technologies such as batteries or supercapacitors [9]. In PEM water electrolysis, water is supplied at the anode side and split into oxygen, electrons and protons. The protons are transported through the polymer electrolyte, while the evolving oxygen is transported out of the cell with the feed water as two-phase flow.

The operating pressure strongly influences the two-phase flow in terms of the evolving volumes. PEM water electrolysis is capable of producing hydrogen safely at a pressurized level of up to 100 bars [7]. A pressurization of 30 bar leads to a small reduction of the electrolysis efficiency in the range of 3% [7,8] due to crossover effects over the membrane. Compared to a additional separate compression up to a pressure of around 30 bar this is still more efficient [7]. A high operating pressure of the electrolysis therefore allows an effective storage and minimizes the costs for following compression steps (if needed).

On the other side an operation at lower pressure levels of the electrolysis cell itself decreases the cell costs, as it allows for a much lighter construction. The profitability of PEM electrolysis is a decisive factor for the future use cases of this process [6] and needs a careful evaluation on the operating conditions. A focus of this work was therefore to find out the influences of different operating conditions, especially of different internal pressures, on the cell performance. Another focus were the two-phase flow processes inside of the GDL at different operating conditions and at different positions on a single GDL.

2. Description of the visualization problem

PEM water electrolysis systems are currently scaled to the megawatt range, necessitating an increase of the active area of an individual cell in order to reduce the overall costs [6]. This scale-up goes along with questions concerning the media distribution on large cell areas. Typically a GDL is used to allow a more homogeneous media distribution along the active cell area. The oxygen side of the GDL provides a cross transport of H_2O to the reactive zone and at the same time an oxygen transport away from the electrode. Of special interest is the information about the oxygen saturation and distribution inside of the GDL, at different points of operation but also at different locations inside a homogeneous GDL. Due to the continuous production of oxygen and hydrogen gas over the whole active area of the electrolysis cell and therefore over the whole contacting area of the GDL, the gases accumulate from the bottom to the top of the electrolysis cell in the case of a vertical orientation. One option to visualize these effects would be to employ a transparent GDL material to allow for optical inspection, yet this approach introduces disturbances to the cell operation, as the electrical connection of the cell has to be carried out by a connection on the side of the cell or otherwise by electrical connectors through the cell. The former leads to a change in the current distribution and the latter leads to a disturbance in the flow field. Therefore a pure optical inspection will introduce perturbations to the observed effects.

3. Solution of the visualization problem

There are methods to allow visualization of the cell structure and the occurring processes inside a cell while at the same time using an unaltered cell setup, employing standard metal-

lic materials as usual for the GDLs and for the surrounding parts like the end plates. One of them is neutron radiography, in which a neutron beam is directed at the cell, and the especially strong neutron attenuation in hydrogen allows visualizing the gas/water distribution. This method has been successfully applied in the past to PEM fuel cells [1,3,4] and liquid fed direct methanol fuel cells [2], where it allowed studying the water distribution inside running cells. This technique has also recently been applied to PEM water electrolysis [5], where the water accumulation on the cathode side was studied. This technique allows investigating the interior of large samples (up to hundreds of cubic centimetres) with a spatial resolution of lower than 100 µm and a temporal resolution of up to 1 s. The ability of neutrons to be transmitted through several centimetres of metal on the one hand and to be very sensitive to small amounts of light elements such as hydrogen, boron and lithium on the other hand makes neutron radiography a unique method for non-destructive testing in both industry and materials science. Using this method, the gas/water distribution inside a PEM water electrolysis cell was studied using neutron radiography at CONRAD-2 (Helmholtz-Zentrum Berlin) for different operation conditions, examining especially the dynamics in the transport and quantifying the distribution along the cell area and the oxygen content of the cell. To the knowledge of the authors this technique is employed for the first time for visualizing the flow processes during PEM water electrolysis on the anode side at different locations of a GDL.

4. Experimental Setup

All measurements were carried out at the CONRAD-2 beamline at the BER II neutron source at Helmholtz-Zentrum Berlin using the following experimental conditions: detector system (sCMOS camera "Andor NEO") with pixel size of 22µm, scintillator screen (^{6}LiFZnS) with a thickness of 100 µm and beam collimation ratio (L/D) of 350. The polymer electrolyte membrane water electrolysis cell was placed in the neutron beam. Images were taken every second. Therefore dynamics in the range of some seconds are visible whereas dynamics faster
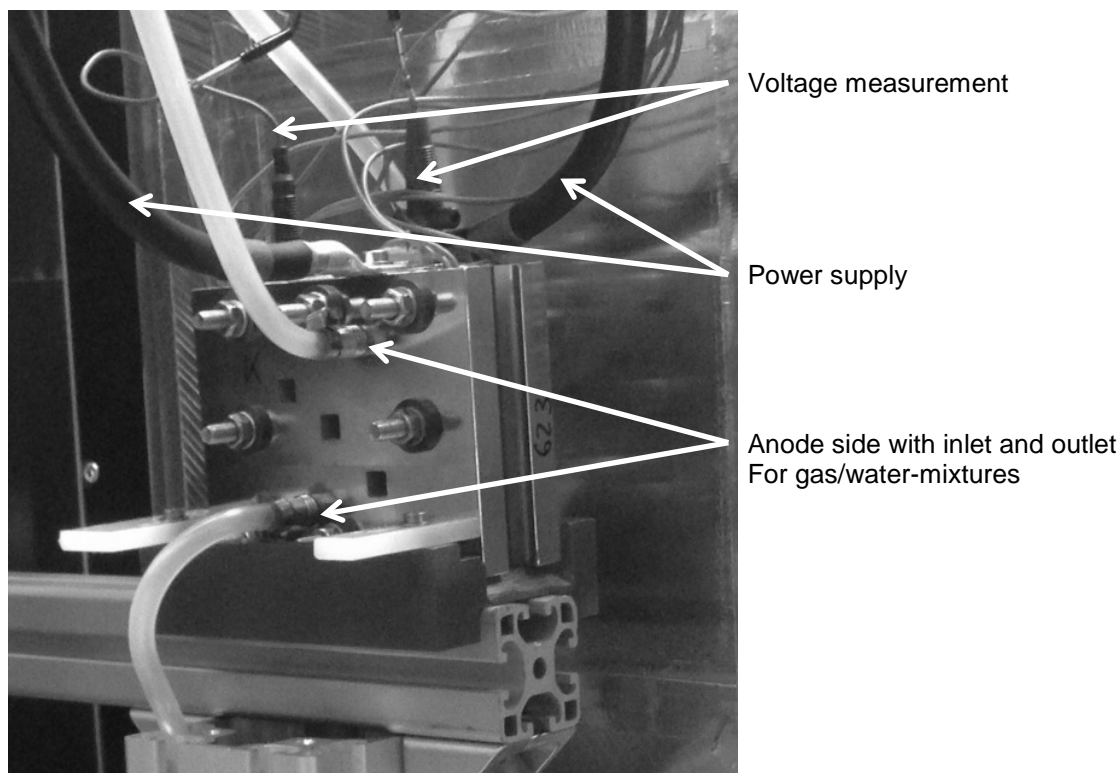
Figure 1: Experimental setup at CONRAD

than 1 s cannot be resolved. The setup consists of an electrolysis cell, which is a machined metal structure. Water and – if needed for the reproduction of boundary conditions on a large cell area – oxygen gas is pumped through the cell. Only the anode side was supplied with water and additional gas, the cathode side was not supplied with water. The cell installed in front of the detector is shown in **Figure 1**. On the cathode side a graphite paper was installed as gas diffusion layer. The resulting measurements are a superposition of anode and cathode side. The processes on the cathode side are not as dynamic as on the anode side due to the missing water circulation and the much thinner gas diffusion layer (around 0,3 mm) compared to the anode side (around 7 mm). Thus the effects due to water fluctuations on the cathode side can be neglected. The cells active area was 42mmx42mm, which is equal to the size of the gas diffusion layer in the setup. The cell was operated at atmospheric pressure. The flow rate of water could be adjusted. The flow was directed from the bottom to the top of the cell. To simulate pressurized conditions, where the evolving gas volumes are smaller, the measurements are done at low current densities to simulate the low gas potion. The effect of the changes in gas density and kinematic viscosity on the dynamics of the two-phase flow has been neglected (see for example [10]). For the effect of pressure on the surface tension on the oxygen/water-interface no measurements could be found. Similar measurements of the combinations water/CO_2 [12][14] and water/methane [13] indicate, that for the given conditions the influence was small and in the range of -10% for water/CO_2 and about -7% for water/methane.
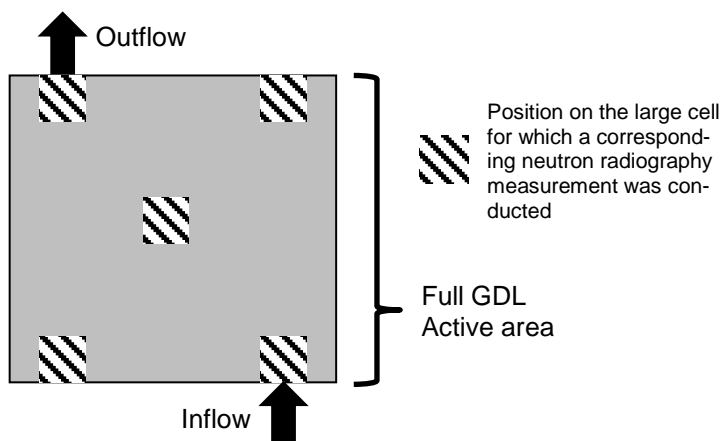
Figure 2: Positions on the large area cell corresponding to the neutron radiography measurements

The inlet and outlet flows are being distributed over the width of the cell before the flow is entering the cell. There is no separate flow field in the cell, as the gas diffusion layer provides the flow field functionality. The gas diffusion layer itself is composed of several layers of stretched metal mesh sheets. The electrical current is distributed from the end plate to the roughest layer with only a small number of contact points to the finest layer with a much higher number of contact points over the sample.

The results of the measurements are images with different greyscale values, representing the intensities of the transmitted neutron beam on different locations on the image. The intensity depends mostly on the amount of water irradiated, as the neutron attenuation in our setup is mainly due to water. An oxygen bubble evolving in water therefore leads to an increase in neutron transmission as the amount of water to the neutron beam to penetrate decreases, as does the neutron attenuation. Hence the oxygen bubbles lead to brighter spots in the image. A reference image (index R) was chosen where the cell is just perfused by water and not applying a current to the cell, so without electrolysis operation. This reference picture R is an averaged picture over 120 single pictures. In order to obtain a measure for the change in the amount of gas between two settings, all images (index M) were divided by the reference image R. The beam attenuation over a thickness z of a material is given by the Beer-Lambert law

$$I_M(i,j) = I_0(i,j) \cdot \exp(-\alpha \cdot z)$$

where $I_0(i,j)$ is the initial beam intensity at the pixel location (i,j), $I_M(i,j)$ is the beam intensity after transmission through the cell and thus through the mixture of water and gas, α is the attenuation coefficient. In order to quantify the change in the water/gas ratio, this intensity $I_M(i,j)$ is divided by the reference intensity $I_R(i,j)$, and solving the resulting equation for the thickness z therefore yields information about the gas volumes $V_{gas}(i,j) = \Delta x \cdot \Delta x \cdot z$ at the the pixel location (i,j), so that

$$V_{gas}(i,j) = \frac{\Delta x^2}{\alpha} \cdot \ln(\frac{I_M(i,j)}{I_R(i,j)})$$

The attenuation coefficient α is composed of the attenuation coefficients of the water, of the gases, and the remaining cell components, so that $\alpha = \alpha_{H_2O} + \alpha_{O_2} + \alpha_{components}$. As the neutron attenuation primarily occurs in the hydrogen of water, only the contribution by water is considered, so $\alpha = \alpha_{H_2O}$. In the work here, a value of α = 5,2 cm^{-1} was determined by a calibration measurement for a defined distance of 5 cm between the measurement setup and the detector.

5. Results

Neutron radiography measurements were conducted for different operating conditions of the testing cell. Those conditions reflect the conditions inside a complete electrolysis cell with an active area of 1.400 cm^2 (at 35 bar) and 15.000 cm² (atmospheric) respectively at different positions of this area (**Figure 2**) and at different current densities. An additional injection of oxygen from the bottom of the measurement cell has been used to reproduce the accumulation of oxygen from the bottom of the cell to the top. This setup therefore allows to study the gas/water distribution and transport, as it would occur in a large area electrolysis cell.

5.1. Comparison between pressurized and atmospheric operation

In a first step some of the points of operation are shown at their corresponding position inside of a larger GDL. The focus was on the normal point of operation for an atmospheric and a simulated pressurized system (35 bar). **Figure 4** shows the comparison at 5 different points of a bigger GDL. One has to keep in mind, that due to a drop in surface tension at higher pressure (see 4) the evolving bubbles might be of a smaller and finer distributed character. At atmospheric operation, strong differences between inlet and outlet are obvious due to the accumulation of larger gas volumes compared to the simulated pressurized operation.
In **Figure 5** two comparisons concerning the O$_2$ content in the open GDL volume (volume of the GDL available for water and gas) are shown.
The pressurized operation is - with focus on the O$_2$ content - nearly independent from the O$_2$ input volume flow (left picture). This correlates with the observations during operation. Gas bubbles mostly grow until a specific size is reached, depending on the structure of the GDL. Then by their own buoyancy they are driven out of the cell. The duration of accumulation is 2-3 seconds depending on the current density. The gas content in the cell in pressurized operation fluctuates in a range of about ±10-15%.
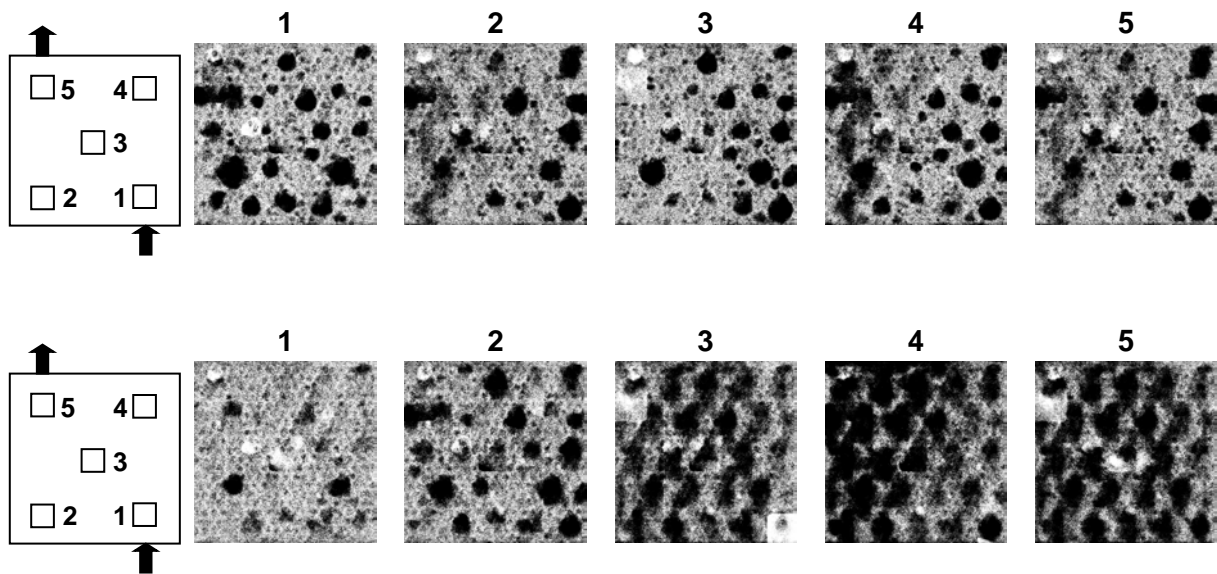
Figure 3: Comparison of the oxygen saturation at a simulated pressurized (35 bar, top pictures) and atmospheric (bottom pictures) operation. Gas is marked in black color
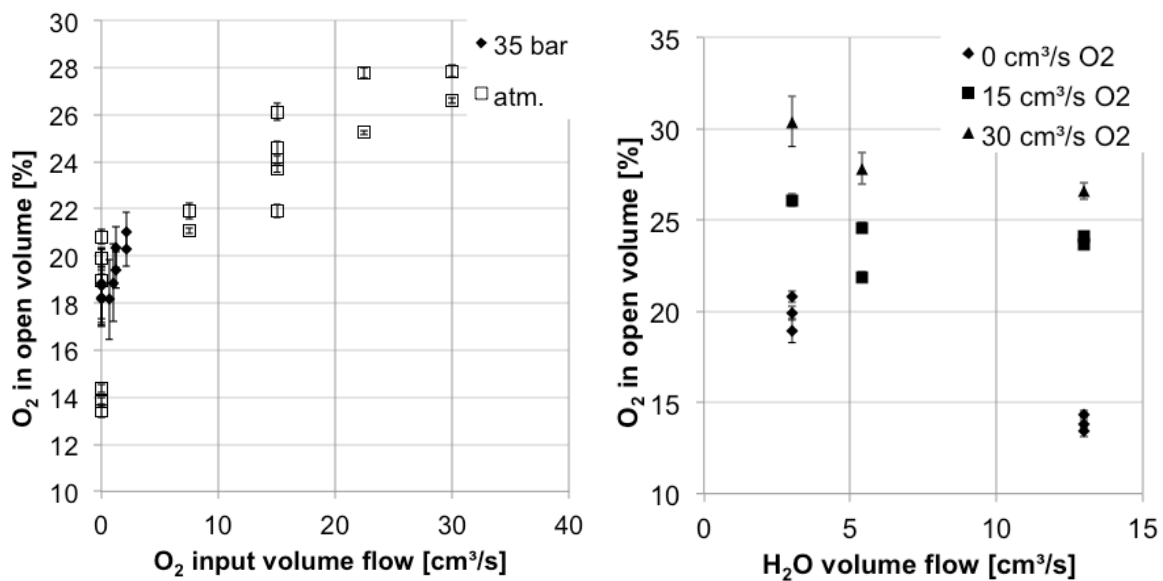
Figure 4: O_2 content in open GDL volume in dependence of O_2 input flow (left) and H_2O input flow (right)

In an atmospheric operation the volumetric O_2 flow is much higher, which leads to a strong dependence between the O_2 input volumetric flow and the gas content inside of the cell. The variations in the gas content are in the range of ± 1-3% of the mean value. Due to the higher gas content, a more steady flow situation arises, which leads to a smaller variation. This is independent from the observation of strongly different gas contents of the sample cells depending on the position in the larger GDL (see **Figure 4**).

The right diagram of **Figure 5** shows the dependence of the O2 content in the open GDL volume from the H_2O input volume flow. In the tendency it shows lower O_2 contents with rising H_2O volume flows.

5.2. Influence of gas fraction on the static point of operation

In **Figure 5** the gas content in the cell is put in relation to the cell voltage for different points of operation, which means also different H_2O and O_2 input volume flows. A relation to the cell performance comparable to the "dry-out" - effect, which is common for fuel cells at high current densities (see for example [11]), could not be observed. The cell performance seems to be independent from the gas content inside of the cell and thereby also from the location inside a bigger gas diffusion layer, at least for the chosen conditions (which lead to a maximum O_2 content of about 30%).

But a difference could be identified in the dynamic behaviour of the voltage at current density jumps in atmospheric operation.
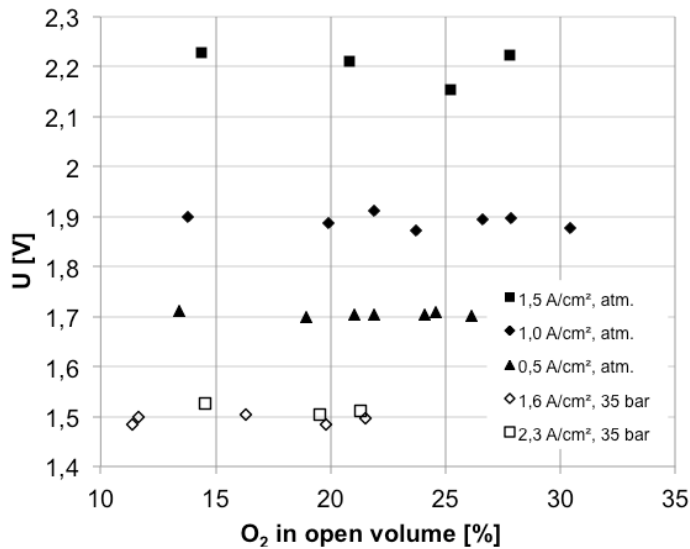
Figure 5: Cell voltage in dependence of the O2 content

5.3. Comparison of the dynamic behaviour

In **Figure 7** the cell voltage after a change in current density is shown for the atmospheric cell operation. The current density was changed from 0,5 A/cm² to 1 A/cm² (dotted lines) and from 1 A/cm² to 1,5 A/cm² (solid lines). The operating state changes have been different concerning water volume flow and oxygen volume flow. It can be seen that there are strong differences concerning the dynamic behaviour. At the step from 0,5 to 1,0 A/cm² the point of operation reaches nearly immediately a steady state, while at the step from 1,0 to 1,5 A/cm² the point of operation needs at least 20 min to reach a quasi-steady state. The reason for this behaviour is up to now unclear and needs further investigation. One possibility is a lack of running-in time. Other measurement setups of the authors have shown a similar behaviour during the running-in-time. But still after 10 hours of operation the situation did not change. No tendency to a decrease during continuous operation of the cell could be identified (see **Figure 6**, small diagram). The lack of per-
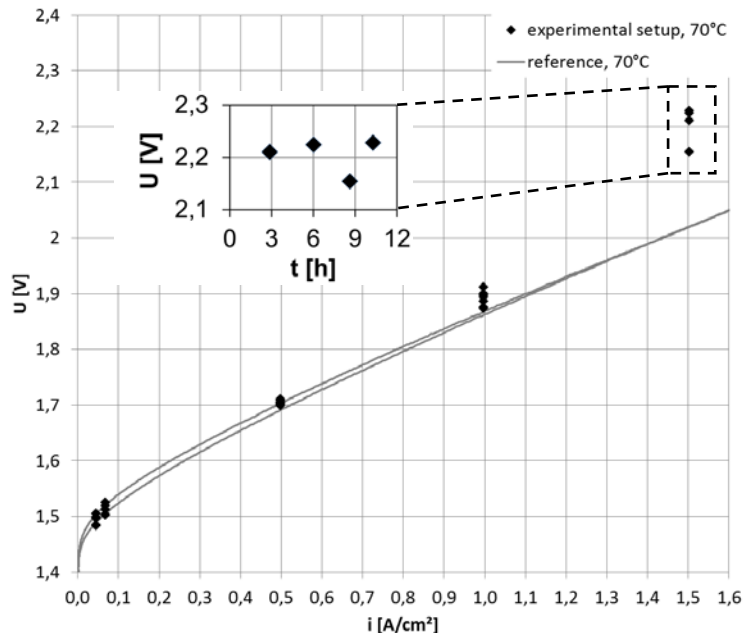
Figure 6: Current - voltage - characteristic of the setup

formance could therefore also arise due to transport problems in the cell at higher current densities and atmospheric operation.
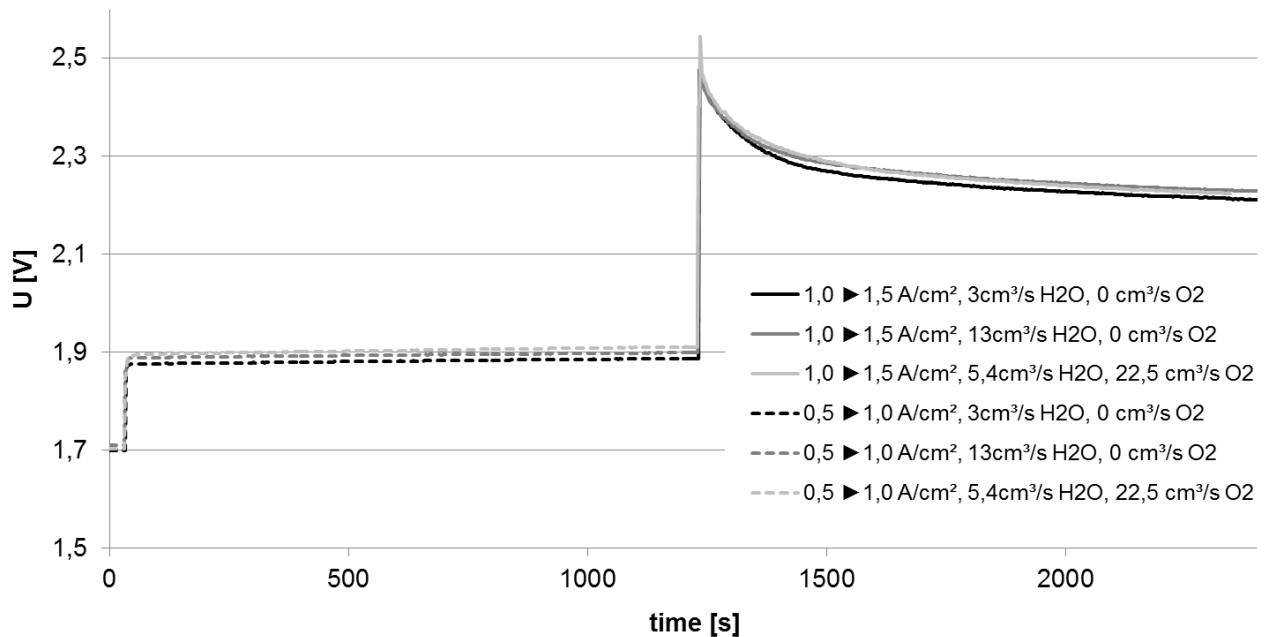
Figure 7: Voltage over time at different atmospheric conditions

5.4. Conclusions

In the present experiment at Helmholtz-Zentrum Berlin, different conditions within a larger GDL area were simulated in order to get an overview over the two-phase flow inside of the GDL. It was found that the two-phase flows depends heavily on the location of the sample (inlet, outlet, center of the GDL) for atmospheric conditions, while at pressurized conditions no significant differences could be observed. The volumes of oxygen were estimated by a comparison of the resulting flow pictures and showed average oxygen contents of about 18 to 20% for pressurized operation and 14 to 30 % for atmospheric operation.

It was seen, that the character of the flow field is nearly equal for different positions inside a GDL at quasi-pressurized conditions (**Figure 4**, top pictures), and the fluctuations in oxygen saturation are in the range of 10-15%. For atmospheric operation the character of the flow field depends strongly on the position inside a GDL (**Figure 4**, bottom pictures), but the oxygen saturation revealed to be more constant with deviations of just 1-3%.

It was also seen that for a steady operation (after about 20 min) the cell voltage is not dependent on the gas content in the open volume up to the gas content levels we could reproduce. But in dynamic operation there is a significant difference between jumps from 0,5 to 1,0 A/cm² and 1,0 to 1,5 A/cm² for the voltage at atmospheric operation. Here a connection to the short running-in time of the cell cannot be excluded. For a definitive statement it would need further investigation with concentration on this aspect.

5.5. Acknowledgements

5.6. Literature

[1]   Satija, R.; Jacobson, D.; Arif, M. & Werner, S., In situ neutron imaging technique for evaluation of water management systems in operating PEM fuel cells, *Journal of Power Sources* , **2004***, 129*, 238 - 245

[2]   Schröder, A.; Wippermann, K.; Lehnert, W.; Stolten, D.; Sanders, T.; Baumhöfer, T.; Kardjilov, N.; Hilger, A.; Banhart, J. & Manke, I., The influence of gas diffusion layer wettability on direct methanol fuel cell performance: A combined local current distribution and high resolution neutron radiography study, *Journal of Power Sources* , **2010***, 195*, 4765 - 4771

[3]   H. Markötter, I. Manke, R. Kuhn, T. Arlt, N. Kardjilov, M. P. Hentschel, A. Kupsch, A. Lange, C. Hartnig, J. Scholta, J. Banhart: Neutron tomographic investigations of water distributions in polymer electrolyte membrane fuel cell stacks, *Journal of Power Sources,* **2012**, 219, 120-125.

[4]   A. Santamaria, H. Y. Tang, J. W. Park, G. G. Park, Y. J. Sohn: 3D neutron tomography of a polymer electrolyte membrane fuel cell under sub-zero conditions, *International Journal of Hydrogen Energy*, **2012**, 37, 10836-10843.

[5]   Selamet, O.; Pasaogullari, U.; Spernjak, D.; Hussey, D.; Jacobson, D. & Mat, M. Two-phase flow in a proton exchange membrane electrolyzer visualized in situ by simultaneous neutron radiography and optical imaging, *International Journal of Hydrogen Energy* , **2013***, 38*, 5823 - 5835

[6]   Marcelo Carmo, David L. Fritz, Jürgen Mergel, Detlef Stolten, A comprehensive review on PEM water electrolysis, *International Journal of Hydrogen Energy*, **2013**, 38, 4901-4934

[7]   Maximilian Schalenbach, Marcelo Carmo, David L. Fritz, Jürgen Mergel, Detlef   Stolten, Pressurized PEM water electrolysis: Efficiency and gas crossover, *International Journal of Hydrogen Energy*, **2013**, 38, 14921-14933

[8]   S.A. Grigoriev, V.I. Porembskiy, S.V. Korobtsev, V.N. Fateev, F. Auprêtre, P. Millet, High-pressure PEM water electrolysis and corresponding safety issues,   *International Journal of Hydrogen Energy*, **2011**, 36, 2721-2728

[9]   Peter D. Lund, Juuso Lindgren, Jani Mikkola, Jyri Salpakari, Review of energy system flexibility measures to enable high levels of variable renewable electricity, *Renewable and Sustainable Energy Reviews*, **2015**, 45, 785-807

[10]   P.J.G. Huttenhuis, J.A.M. Kuipers, W.P.M. van Swaaij, The effect of gas-phase density on bubble formation at a single orifice in a two-dimensional gas-fluidized bed, *Chemical Engineering Science*, **1996**, 51, 5273-5288

[11]   Tibor Fabian, Jonathan D. Posner, Ryan O'Hayre, Suk-Won Cha, John K. Eaton, Fritz B. Prinz, Juan G. Santiago, The role of ambient conditions on the performance of a planar, air-breathing hydrogen PEM fuel cell, *Journal of Power Sources*, 161, **2006**, 168-182

[12]   Luís M.C. Pereira, Antonin Chapoy, Rod Burgass, Mariana B. Oliveira, João A.P. Coutinho, Bahman Tohidi, Study of the impact of high temperatures and pressures on the equilibrium densities and interfacial tension of the carbon dioxide/water system, *The Journal of Chemical Thermodynamics*, Available online 14 May **2015**

[13]   Werner Sachs, Volker Meyn, Pressure and temperature dependence of the surface tension in the system natural gas/water principles of investigation and the first precise experimental data for pure methane/water at 25°C up to 46.8 MPa, *Colloids and Surfaces A: Physicochemical and Engineering Aspects*, 94, **1995**, 291-301

[14]   Mohammad Sarmadivaleh, Ahmed Z. Al-Yaseri, Stefan Iglauer, Influence of temperature and pressure on quartz–water–CO2 contact angle and CO2–water interfacial tension, *Journal of Colloid and Interface Science*, 441, **2015**, 59-64